Hindawi
Scientific Programming
Volume 2021, Article ID 5879255, 9 pages
https://doi.org/10.1155/2021/5879255

Research Article

Therapeutic Effect of Cervical Cerclage on Cervical Insufficiency during Pregnancy Analyzed by Magnetic Resonance Image under Neural Network Algorithm

Yongjuan Liu,[1] **Yongpan Tan**,[2] **Rongxia Liu**,[1] **Xuekui Ye**,[1] **Lina Wang**,[1] **Wei Cui**,[1] **Dan Lu**,[1] **Jing Guo**,[1] **and Dongmei Chu**[1]

[1]*Department of Gynaecology, Shijiazhuang No. 4 Hospital, Shijiazhuang 050000, Hebei, China*
[2]*Department of Medical Imaging and Ultrasound, Shijiazhuang No. 4 Hospital, Shijiazhuang 050000, Hebei, China*

Correspondence should be addressed to Dongmei Chu; 150511135@stu.sxit.edu.cn

Received 7 September 2021; Revised 9 November 2021; Accepted 11 November 2021; Published 21 December 2021

Academic Editor: M Pallikonda Rajasekaran

Copyright © 2021 Yongjuan Liu et al. This is an open access article distributed under the Creative Commons Attribution License, which permits unrestricted use, distribution, and reproduction in any medium, provided the original work is properly cited.

Objective. This research was developed to investigate the effect of magnetic resonance imaging (MRI) analysis based on neural network algorithm for cervical ligation in the treatment of cervical insufficiency. *Methods*. 44 patients who were suspected to be pregnant with cervical insufficiency and needed cervical ligation were selected. MR imaging analysis was performed before cervical ligation. MR images were analyzed based on the back propagation neural network (BPNN) algorithm, and patients were randomly divided into experimental group and control group. Preoperative MRI analysis was performed in the experimental group, while simple transvaginal ultrasonography was used to diagnose cervical insufficiency in the control group. Then, postoperative fetal preservation time, vaginal bleeding rate, and infection rate within one week after surgery were compared between the two groups. *Results*. Based on experience and experimental testing, the relevant parameters were set as follows. The number of particles $n = 50$, the inertia weight $\omega = 0.9$, and $c1 = c2 = 2$. The weight range of the output layer of the neural network was $[-1, 1]$, the target error $e = 10^{-5}$, and the maximum number of iteration steps was 3,000. Compared with the control group, the experimental group's postoperative bleeding rate and infection probability were substantially reduced, while the normal delivery rate was substantially increased ($P < 0.05$). *Conclusion*. MR image analysis based on neural network algorithm played an important role in cervical cerclage surgery. The image map showed the local anatomy clearly, increasing the success rate of the operation and improving the prognosis of the patient.

1. Introduction

Cervical insufficiency is also known as cervical atresia and cervical relaxation. Patients with cervical insufficiency have reduced cervical fibrous tissue, elastic fiber, smooth muscle, and other tissues. Or, the function of the isthmic sphincter may decline due to the fracture of cervical fibrous tissue, causing pathological dilation or relaxation of the cervical opening [1–3]. In patients with cervical insufficiency, the clinical condition of painless cervical dilation observed before the first full month after pregnancy is most likely to cause miscarriage in 0.1–2% [4]. 20–25% of pregnancy interruptions are due to cervical insufficiency. Therefore, the treatment of cervical cancer has received more and more attention [5]. Prior to cervical ligation, the treatment of cervical insufficiency was mainly through the formation of cervical scar tissue or the placement of mechanical support around it to strengthen the cervix [6]. Cervical ligation is currently the only method and effective means for the treatment of cervical cancer uterine [7]. The cervical cerclage is to strengthen the tension of the cervical canal as much as possible to prevent the extension of the lower uterine segment and the dilatation of the cervical orifice, so as to assist the cervical orifice in bearing the gravity of the fetus and fetal appendages in late pregnancy. Laparotomy cervical ligation is only applicable to patients who need cervical ligation in the second trimester. In recent years, laparoscopic cervical ligation is becoming more and more popular, and laparoscopic surgical techniques are replacing traditional gynecological laparotomy. Cervical cerclage has achieved remarkable results in the treatment of cervical incompetence and has become the best choice for patients with cervical incompetence.

MRI is an examination method for cervical insufficiency during pregnancy, which is usually used in complex cases and limited ultrasound examination and plays an important complementary role in preoperative evaluation [8]. With the rapid development of artificial intelligence, algorithms are gradually applied to the field of MR images. In recent years, BPNN algorithm and support vector machine (SVM) algorithm are combined with MR image feature analysis. SVM is a new machine learning method proposed by Vapnik et al. [9]. Due to its excellent learning performance, it has become a research hotspot in the field of machine learning and has been successfully applied in many fields such as face recognition, face recognition, handwriting number recognition, and text automatic classification [10, 11]. In summary, the characteristics of traditional MR images of cervical insufficiency during pregnancy are not typical, and there are difficulties in the diagnosis and treatment of the disease [12]. Moreover, misdiagnosis and missed diagnosis will occur in the diagnosis and treatment process. With the continuous development of artificial intelligence and neural network algorithms, new methods have been developed for the analysis of cervical insufficiency in pregnancy [13].

Based on the above reasons, this study was developed based on the neural network algorithm MR image analysis of cervical insufficiency in pregnancy, which aimed to improve the success rate of diagnosis and treatment of cervical insufficiency in pregnancy. It was hoped to provide evidence for imaging analysis and automatic diagnosis of cervical insufficiency.

2. Methods

2.1. Research Objects

2.1.1. General Information. A total of 44 patients with cervical insufficiency in the hospital from December 2018 to April 2020 were selected. There were 28 primiparas and 16 puerpera aged between 24 and 38 years. Gestation was 12^{+4} to 26^{+3} weeks. All subjects were randomly rolled into experimental group and control group, with 22 people in each group. Patients in the experimental group were confirmed by B ultrasound diagnosis, who received the cervical circumcision after pelvic MRI examination. Patients in the control group were confirmed by B ultrasound, and cervical circumcision was performed directly. This study had been approved by the Ethics Committee of the hospital, and all patients had signed the informed consent.

2.1.2. Inclusion and Exclusion Criteria. The inclusion criteria were as follows: patients who aged over 18 years old and were diagnosed with cervical insufficiency according to the diagnostic criteria and the patients who signed the informed consent, and this study was approved by the Committee of Ethics and Management of hospital.

The exclusion criteria were as follows: patients younger than 18 years old, patients with other reproductive systems or unable to receive cervical ligation, patients who did not cooperate with the examiner, and patients with incomplete data.

2.1.3. Diagnostic Criteria for Cervical Insufficiency. (a) In the second trimester, when there were no obvious contractions, the width of the fallopian tube as measured by transvaginal ultrasound was greater than 0.6 cm. (b) The width of the internal opening of the cervix was greater than 1.5 cm. (c) The length of the cervix was less than 2.5 cm, and the length of the cervix more than 3 cm was normal. A length of less than 2 cm indicated a substantially shortened cervix, indicating possible miscarriage or preterm labor. (d) Whether there was a visible amniotic sac in the blood vessels of the cervix, with or without embryos, was diagnosed based on the above two standards.

2.2. Inspection Methods. 3.0 T MRI equipment was employed. There was no need to clean the colon, and no objects can be placed in the rectum or vagina during the examination. The patient was supine, and the area from the inlet of the pelvis to the symphysis pubis was scanned. Sequential images were generated using the Turbo Spin-Echo (TSE), T1WI, and T2WI. The imaging azimuthal included horizontal, sagittal, and coronal positions. Horizontal axis point TSE-T1WI fat parameters were TR/TE = 500MS/21MS, reconstruction matrix of 320×256, FOV of 220×220 mm, thickness of 3 mm, layer interval of 0.6 mm, layer number of 30, and NEX1. TSE-T1WI sequence parameters of the horizontal axis were TR/TE = 500MS/21MS, reconstruction matrix of 320×256, FOV of 220×220 mm, thickness of 3 mm, layer spacing of 0.6 mm, layer number of 30, and Nex1. Oblique axis position TSE-T2WI sequence parameters were TR/TE = 5000MS/91MS, reconstruction matrix of 320×256, FOV of 220×220 mm, layer thickness of 3 mm, layer spacing of 0.6 mm, layer number of 30, and NEX 1. TSE-T2WI serial parameters were TR/TE = 4270MS/97MS, reconstruction matrix of 448×358, FOV of 200×200 mm, layer thickness of 3 mm, layer spacing of 0.6 mm, layer number of 25, and NEX 1.

2.3. MR Image Analysis Based on Neural Network Algorithm. The MR image analysis based on the BP neural network algorithm is as follows. For the evaluation of MR images based on neural network algorithms, the neural network algorithm has to go through the following steps. The first is initializing the network. The input and output of the neural network are composed of a series of input nodes designated as (X, Y). According to the number of these input nodes, the number of nodes in the input layer, hidden layer, and output layer of the network is determined. Then, the continuous value and the threshold are initialized, and the continuous weight ω_{ij} between the input layer and the neural layer is established in the hidden layer, which are the thresholds of the hidden layer and output layer of A and B, respectively. Finally, the exciting neuron function $f(x)$ and learning speed η of the neural network are calculated.

According to the input variable X in the neural network, the continuous weight ω_{ij} between the input layer and the hidden layer, and the threshold α of the hidden layer, the output H of the hidden layer is obtained.

$$H_j = \sum_{i=1}^{n} \omega_{ij} x_i - a_j \; j = 1, 2, l. \tag{1}$$

In the above equation, f is the activation function of the hidden layer and l is the number of nodes in the hidden layer. There are many forms to express the excitation function, including the following one.

$$f x = \frac{1}{1 + e^{-x}}. \tag{2}$$

According to the output H in the hidden layer calculated in the previous step, the hidden layer is bound to the output value of the continuous weight ω_{jk} and the threshold b, and the prediction of the output of the O_{32} neural network is obtained.

$$O_k = \sum_{i=1}^{l} H_j \omega_{jk} - b_k \, b = 1, 2, m. \tag{3}$$

The output value Y in the neural network and the network output value O obtained in the previous step are used to calculate the prediction error e.

$$e_k = Y_k - O_k \, k = 1, 2, m. \tag{4}$$

The connection weights ω_{ij} and ω_{jk} of the neural network are calculated according to the predicted value e of the neural network.

$$\begin{aligned} \omega_{ij} &= \omega_{ij} + \eta H_1 \left(1 - H_j\right) x(i) \sum_{k=1}^{m} \omega_{jk} e_k \quad i = 1, 2, n; \, j = 1, 2, l, \\ b_k &= b_k + e_k \quad k = 1, 2, m. \end{aligned} \tag{5}$$

It is judged whether the end condition of the algorithm iteration is satisfied, if not, return to step two.

SVM is a feedforward neural network, which can make the longest distance between the two samples on both sides of the plane with the shortest distance from the plane. Versatility, robustness, and simple calculation are all the advantages of support vector machines, and they also have the characteristics of theoretical perfection and effectiveness. The key to constructing the support vector machine neural network algorithm is the inner product kernel between the “support vector” $x(i)$ and the vector x extracted from the input space. The types of kernel functions included are as follows:

$$\begin{aligned} K(x, x_i) &= x^T x_i, \\ K(x, x_i) &= \exp(-\gamma x - x_i) \, \gamma > 0, \\ K(x, x_i) &= \left(\gamma x^T x_i + r\right)^p, \\ K(x, x_i) &= \tanh\left(\gamma x^T x_i + r\right). \end{aligned} \tag{6}$$

The C-SVC model is a relatively common two-category support vector machine model, and its specific manifestations are as follows.

$$T = \{(x_1, y_1), \Lambda, (x_1, y_1)\} \in (X \times Y)^l. \tag{7}$$

The appropriate kernel function $K(x, x_i)$ and the appropriate parameter C are selected to construct and solve the optimization problem.

$$\min \frac{1}{2} \sum_{i=1}^{j} \sum_{j=1}^{i} y_i y_j - \sum_{j=1}^{t} a_j 0 \leq \alpha_i \leq C. \tag{8}$$

2.4. Operations. After a series of preoperative preparations, prophylactic cervical ligation was carried out. Diagnosis required before or during pregnancy was incomplete, and there was no obvious cervical dilation or abortion warning during pregnancy. In an evaluation of the patient’s preoperative general condition, the circular cervical ligation in the lower abdomen was appropriate for those who cannot be ligated through the vagina. It was because they had not had a salpingectomy (such as cervical shortening, extensive cervical excision, and cervical scarring). Of these, 27 patients underwent transvaginal cervical circumcision, and 15 patients underwent transabdominal cervical circumcision.

After a vaginal vasectomy, a classic neck bandage was performed. Lumbar anesthesia combined with epidural anesthesia was applied. The body part was bladder surgery part. Iodophor was used to fully disinfect the vulva, vagina, and cervix. The vaginal hook was used to completely expose the cervix and the posterior dome. When the bladder meridian tissue was torn, the cervix and bladder were torn in reverse. A double strand of thread (number 10) was taken, starting at the 11 o’clock point of the cervix and going through about two-thirds of the muscle layer. The thickness was about 0.5 cm–0.8 cm wide, and the mucous membrane should be avoided. A 0.2 cm–0.3 cm rubber tube was put on it after the needle was released, and the cervix was sutured at 1, 5, and 8 o’clock. Then, the needle went out in the cervix 1 o’clock direction, and the tightness was adjusted in the cervix 11 o’clock direction, knotting in the anterior fornix of the vagina.

The anesthesia used in laparoscopic cervical ligation was general anesthesia. The patient was supine on the operating table during the operation. Four trocars were placed on the lower abdomen and on either side of the navel and then operated through a laparoscope and an operating device. First, the retroflexion of the bladder was opened, the bladder was gently pushed, and the suture was straightened with the Mersilene band. There were needles at each end of the Mersilene belt, and the needles at each end passed from the posterior side of the uterus in front of the broad ligament and passed at the junction of the cervical and sacral ligaments, where there were no blood vessels. Given that the uterus was relatively large in the second trimester, the patient tilted to the other side when the procedure was performed on one side. In this way, the surgical field of vision and operation range were expanded, and some unnecessary injuries were avoided. At the end of the procedure, it was checked if the Mersilene band was in the right place that was the internal opening of the cervical canal. Then, it was necessary to check whether there were fallopian tubes, ovaries, and other tissues in the ring tie band. After confirmation, the ring tie was adjusted to the front of the uterus and tied firmly more than four times.

2.5. Observation Indexes. Postoperative conditions were observed, including postoperative fetal preservation time, vaginal bleeding rate within one week after surgery, premature rupture of membranes, and infection rate. It was checked whether miscarriage occurred after surgery and the number of weeks of delivery for those who had not miscarried. The newborn's weight was measured at one minute after birth.

2.6. Statistical Analysis. In this study, SPSS 22.0 was used for data processing. Measurement data were expressed as mean ± standard deviation, and counting data were expressed as %. The general data of the two groups of patients were comparable, and there was no significant difference, $P > 0.05$. $P < 0.05$ indicated that the difference was statistically considerable.

3. Results

3.1. MR Image Analysis Results Based on BPNN Algorithm. The middle layer of the BPNN structure with a single hidden layer uses the sigmoid function as the transfer function and the linear transfer function as the output layer. If it is the number of neurons in a single hidden layer, the automatic adjustment method is usually selected, such as the hidden layer of the short axis network with the number of neurons between two to eight and the long axis of two to five neuron hidden layer. Because the BP algorithm was used and it had convergence speed, the local fitting method was usually selected to complete the experiment in the training of neural networks. Since the time of global fitting required more than seven hours, it was seldom used. The image of cervical insufficiency during pregnancy is illustrated in Figure 1.

Four algorithms BPNN, PSO-BPNN, APSO-BPNN, and PIPSO-BPNN were used to carry out a series of classification simulations in MATLAB7.0 environment. Based on experience and experimental testing, the relevant parameters were set as follows: the number of particles $n = 50$, the inertia weight $\omega = 0.9$, and $c1 = c2 = 2$. The weight range of the output layer of the neural network was $[-1, 1]$, the target error $e = 10^{-5}$, and the maximum number of iteration steps was 3,000. A threefold cross-validation method was used to select training samples and test samples. Before classification, the signal-to-noise ratio was used to reduce the dimensionality of the attributes of the data set. The relationship between dimension and classification error rate is illustrated in Figure 2.

The average classification accuracy of the four algorithms on the three types of datasets pima, wdbc, and balance is illustrated in Table 1, and the number of iterations of PSO and BP on the three types of datasets of the four algorithms is illustrated in Table 2.

3.2. MR Image Analysis Based on SVM Neural Network Algorithm. The forward test data of time nodes $t = 6, 8, 9, 12$, and 17 generated by the LV simulator were used for comparison experiments. The time nodes of sampling time included 6 and 12. The rest were non-sampling time. The image of cervical insufficiency during pregnancy is illustrated in Figure 3.

The global displacement field fitting method with $C = 4$ and $\gamma = 0.2$ without edge points was selected as the fitting method. When the conditions were set for stopping Newton iteration, the difference between the results of the two iterations was smaller than the threshold ε, usually, $\varepsilon = 10^{-4}$. After three Newton iterations, the stop condition was generally reached, which indicated that the designed calculation model had good convergence. The experimental results using SVM are shown in Table 3.

Obviously, regardless of the mean square error (mse-x, mse-y, and mse-z) or the maximum predicted displacement error (err-x, err-y, and err-z), good experimental results were obtained by using SVW. The mean square error was below 0.08 cm, and some mean square error was even on the order of 10^{-3}. Therefore, it was successful, feasible, and satisfactory to use the SVM method to calculate the cervical insufficiency during pregnancy. Compared with some foreign deformation calculation methods, the error was generally 0.06–0.09 cm, so the SVW-based method proposed was still effective.

3.3. Preservation Time after Cervical Cerclage. In the two groups of patients after transvaginal cervical cerclage or laparoscopic cervical ligation, the experimental group had an average postoperative fetal preservation time of (8.9 ± 3.8) days, and the control group had an average postoperative fetal preservation time of (7.8 ± 5.1) days. The postoperative fetal preservation time of the two groups of patients was compared, and the difference was statistically considerable, $P < 0.05$ (Figure 4).

3.4. Vaginal Bleeding Rate within One Week after Surgery. There were 22 patients in the experimental group, 7 patients were with postoperative bleeding, and the bleeding rate was 31.8%. There were 22 patients in the control group, and 9 patients (40.9%) were with postoperative bleeding. The vaginal bleeding rate within one week after the operation of the two groups of patients was compared, and the difference was statistically considerable, $P < 0.05$ (Figure 5(a)). Among the seven patients with bleeding in the experimental group, four patients had a bleeding volume of no more than 300 mL, two patients had a bleeding volume of 500 mL, and one patient had a bleeding volume of 800 mL. In the control group, five patients had a bleeding volume of less than 300 mL, three patients had a bleeding volume of 500 mL, and one patient had a bleeding volume of more than 800 mL, as illustrated in Figure 5(b).

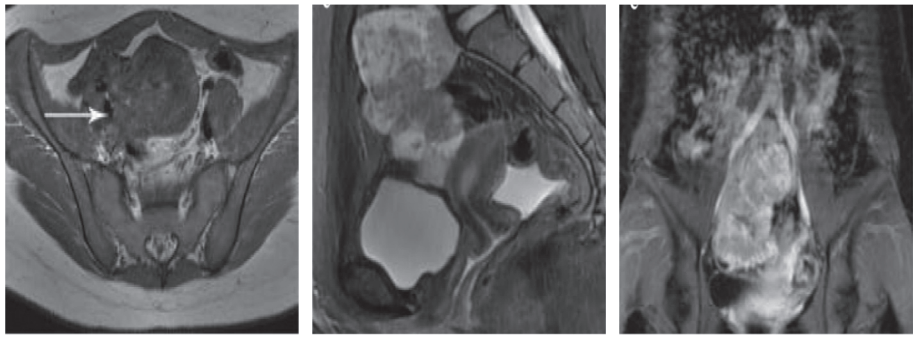

Figure 1: MR images of cervical insufficiency during pregnancy based on the BPNN algorithm.

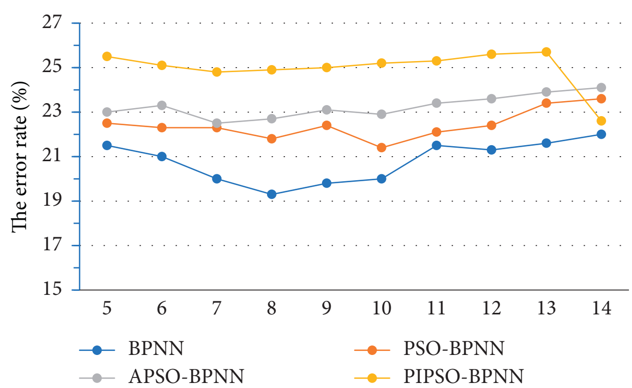

Figure 2: The relationship between dimensionality and classification error rate in the four algorithms.

Table 1: The average classification accuracy of the four algorithms.

Data set	BPNN (%)	PSO-BPNN (%)	APSO-BPNN (%)	PIPSO-BPNN (%)
Pima	91.9	93.2	94.8	86.4
Wdbc	87.3	87.9	91.7	92.3
Balance	86.8	87.4	86.8	92.4

Table 2: Number of iterations of PSO and BP.

Algorithm	PSO	BP
BPNN	—	4000
PSO-BPNN	340	3800
APSO-BPNN	290	3000
PIPSO-BPNN	65	2500

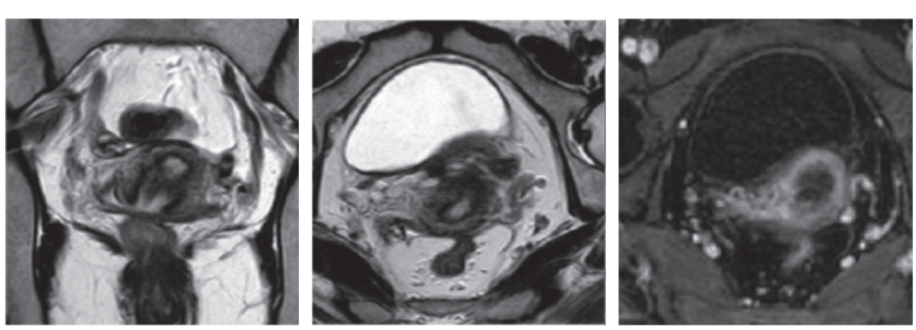

Figure 3: MR images of cervical insufficiency during pregnancy based on SVM neural network algorithm.

Table 3: Deformation calculation results based on SVM.

Time node	Running time	Mse-x	Mse-y	Mse-z	Err-x	Err-y	Err-z
6	1600	0.0783	0.0235	0.0256	0.0345	0.0257	0.0863
8	1600	0.0356	0.0524	0.0258	0.0162	0.0256	0.0872
9	1600	0.0245	0.0352	0.0258	0.0367	0.0366	0.0363
12	1600	0.0523	0.0746	0.0753	0.0267	0.0268	0.0289
17	1600	0.0759	0.0267	0.0279	0.0367	0.0257	0.0278

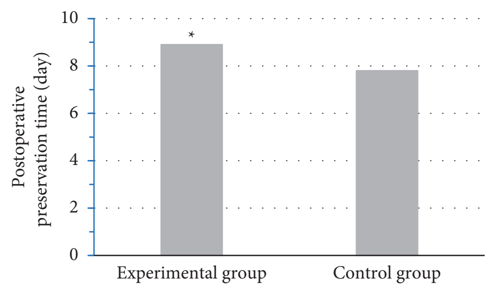

Figure 4: Comparison of postoperative fetal preservation time between the two groups. *Note.* *indicates significant differences, $P < 0.05$.

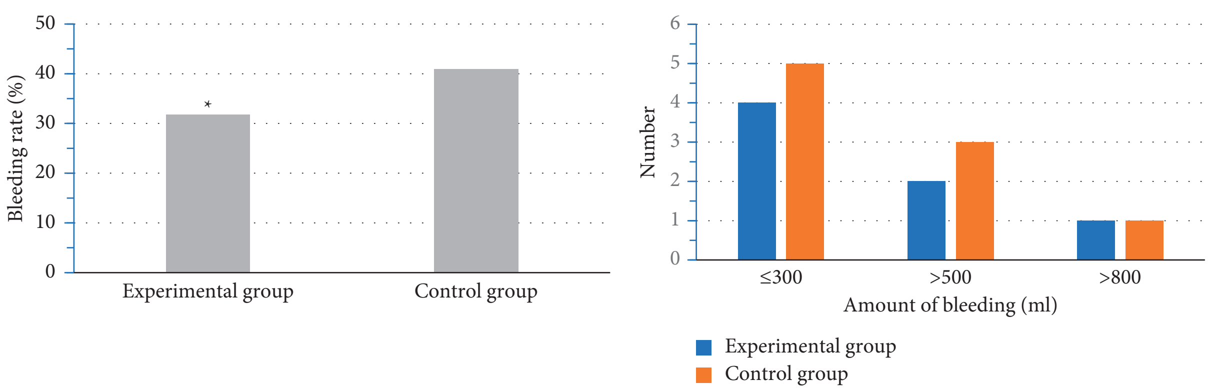

(a) (b)

Figure 5: (a) Comparison of bleeding rate within one week after operation between the two groups. *Note.* *indicates significant differences, $P < 0.05$. (b) The bleeding volume of the two groups of patients within one week after surgery.

3.5. Incidence of Infection. After the two groups of patients underwent vaginal cervical cerclage or laparoscopic cervical ligation, six patients in the experimental group developed infections after the operation, and the incidence of premature rupture of membranes was 27.3%. A total of seven patients in the control group had premature rupture of membranes, and the rate of premature rupture of membranes was 31.2%. The difference was statistically considerable, $P < 0.05$, as illustrated in Figure 6.

3.6. Postoperative Pregnancy Outcome. There were a total of 22 patients in the experimental group, the number of weeks of delivery was 32.4 ± 4.3 gestational weeks, and 2 cases had late abortion at 15^{+4}–21^{+2} gestational weeks. Two patients were delivered prematurely at 29^{+4} and 31^{+6} gestational weeks, respectively, and 18 patients were delivered at 37^{+2}–38^{+6} gestational weeks. In the control group, the number of weeks of delivery was 31.9 ± 5.7 gestational weeks, and 4 patients had late miscarriage at 15^{+5}–22^{+5} gestational weeks. Three cases had preterm births at 31^{+4}, 29^{+6}, and 30^{+4} gestational weeks, respectively, and 13 patients had normal delivery at 37^{+2}–38^{+5} gestational weeks, as illustrated in Figure 7. The normal delivery rate of the experimental group was 81.2%, and that of the control group was 59.1%. The postoperative pregnancy outcomes of the two groups were compared, and the difference was statistically considerable, $P < 0.05$. The postoperative pregnancy outcome of the two groups of patients is illustrated in Figure 7.

4. Discussion

Cervical insufficiency is one of the causes of recurrent abortion and premature delivery in late pregnancy, accounting for about 15% of recurrent abortion in the second trimester [14]. Because of this huge data, people gradually pay attention to these diseases of cervical insufficiency. Although the pathologic mechanism of this disease is not

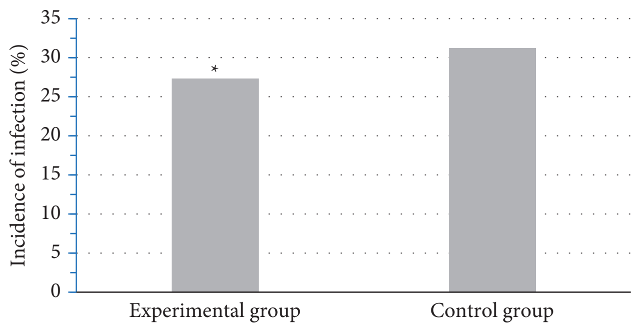

Figure 6: Probability of postoperative infection in the two groups. *Note.* *indicates significant differences, $P < 0.05$.

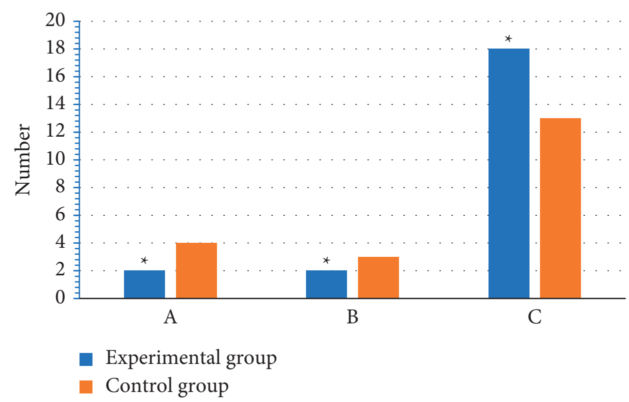

Figure 7: Comparison of postoperative pregnancy outcomes between the two groups (A: abortion in the third trimester, B: premature delivery, and C: normal delivery). *Note.* *indicates significant differences, $P < 0.05$.

clear, the recognized causes include congenital uterine abnormalities, acquired labor induction history, gynecological inflammation, and history of cervical surgery. All these will lead to the gradual loss of sphincter function in the cervical isthmus, which eventually become pathological cervical relaxation [8]. The mechanism of cervical ligation is mainly increasing the tension of the cervical canal to prevent the dilation of the cervix and the extension of the lower part of the uterus, and the operation can help the cervix to share some pressure load brought by the fetus [15].

In this study, BPNN was innovatively applied to the MRI imaging detection of cervical function before cervical ligation, and the effectiveness of the MRI image based on BPNN algorithm in the treatment of cervical incompetence was analyzed. First, the initialization network, the neural network, and the output were formed into a sequence. After initialization of the continuous weights and thresholds, the neuron excitation function $f(x)$ and the learning rate η of the neural network were given [16]. Then, the SVM neural network algorithm was employed to analyze the MR images, and the inner product kernel between the support vector $x(i)$ and the vector x extracted from the input space was constructed. After the kernel function, the appropriate kernel function $K(x, x_i)$ and the appropriate parameter C were selected to construct and solve the optimization problem. From the experiment of neural network fitting results, it was found that there were no edge points in the training data, and the top and bottom test points were not included in the test data. Generally, a small mean square error was obtained. BPNN, PSO-BPNN, APSO-BPNN, and PIPSO-BPNN were adopted to carry out a series of classification simulations in the MATLAB 7.0 environment. Based on experience and experimental testing, the relevant parameters were set as follows: the number of particles $n = 50$, the inertia weight $\omega = 0.9$, and $c1 = c2 = 2$. The weight range of the output layer of the neural network was $[-1, 1]$, the target error was $e = 10-5$, and the maximum number of iteration steps was 3,000 [17]. BPNN algorithm overcomes the problems of local minima and slow convergence of traditional algorithms, but there is no unified theoretical guidance for the selection of BPNN structure, which can only rely on experience. If the network structure is too large, the training efficiency is not high, and there may be an overfitting phenomenon, resulting in low network performance and reduced fault tolerance. If the structure is too small, the network may not converge. The structure of the network directly affects the approximation ability and generalization of the network. Therefore, how to choose the appropriate network structure in application is an important problem. In a word, the MRI based on the BPNN algorithm in this study clearly showed the local anatomical structure, which improved the success rate of surgery and the prognosis of patients.

Cervical ligation is mainly implemented through strengthening the tension of the cervical tube to inhibit the extension of the lower uterine segment and the expansion of the cervical mouth. Cervical ligation can also help the cervix to bear the load of fetal growth in the third trimester to a certain extent [18]. Although cervical ligation is one of the most effective methods recognized by most clinicians for the treatment of cervical insufficiency, there is no unified standard for cervical ligation in the treatment of cervical insufficiency [19, 20]. The results showed that cervical ligation during pregnancy can effectively treat cervical insufficiency. Brown et al. [21] showed that, for pregnant women with typical symptoms of cervical insufficiency, the therapeutic effect of emergency cervical ligation was better than the traditional conservative treatment. This is in line with the results of this study. Our results showed that both prophylactic and emergency cervical ligation can prolong gestational age and improve pregnancy outcomes.

5. Conclusion

In this study, BPNN algorithm and PSO-SVM algorithm were used to analyze the MRI image characteristics of patients with cervical insufficiency during pregnancy. Then, the two neural algorithms were compared to evaluate the therapeutic effect of MRI image features. The algorithm proposed had high continuity and reliability, which also had good segmentation performance, and the diagnosis accuracy of cervical insufficiency during pregnancy was improved. This algorithm not only greatly improved the segmentation efficiency and reduced a large number of manual repetitive operations but also can assist clinicians in the clinical auxiliary diagnosis of other uterine diseases, so it was of high theoretical and practical significance. The shortcoming of this study is that it is found that the training data do not contain edge points and the test data do not contain the top and bottom test points from the comparative experiment of neural network fitting results, and generally, small mean square error is obtained. It may be due to the shortcomings of the neural network algorithm itself, which often cannot get the global optimal solution but can only get the local optimal solution. Therefore, it is recommended to exclude edge points when neural network is used for local fitting in subsequent studies. The problems existing in this study need to be further improved in the follow-up work.

Data Availability

The data used to support the findings of this study are available from the corresponding author upon request.

Conflicts of Interest

The authors declare no conflicts of interest.

Authors' Contributions

Yongjuan Liu and Yongpan Tan contributed equally to this work.

References

[1] I. Kyvernitakis, H. Maul, and F. Bahlmann, "Controversies about the secondary prevention of spontaneous preterm birth," *Geburtshilfe und Frauenheilkunde*, vol. 78, pp. 585–595, 2018.

[2] E. Caspi, D. Schneider, Z. Mor, R. Langer, Z. Weinraub, and I. Bukovsky, "Cervical internal os cerclage: description of a new technique and comparison with Shirodkar operation," *American Journal of Perinatology*, vol. 7, pp. 347–349, 1990.

[3] N. Garry, O. Keenan, S. Lindow, and T. Darcy, "Pregnancy outcomes following elective abdominal cerclage following cervical excision surgery for neoplastic disease," *European Journal of Obstetrics & Gynecology and Reproductive Biology*, vol. 256, pp. 225–229, 2021.

[4] E. Saridogan, O. P. O'Donovan, and A. L. David, "Preconception laparoscopic transabdominal cervical cerclage for the prevention of midtrimester pregnancy loss and preterm birth: a single centre experience," *Facts, views & vision in ObGyn*, vol. 11, no. 1, pp. 43–48, 2019.

[5] V. Berghella, A. Ciardulli, O. A. Rust et al., "Cerclage for sonographic short cervix in singleton gestations without prior spontaneous preterm birth: systematic review and meta-analysis of randomized controlled trials using individual patient-level data," *Ultrasound in Obstetrics and Gynecology*, vol. 50, no. 5, pp. 569–577, 2017.

[6] Y. Wang, H. Duan, N. Zhang, S. Wang, and L. Gao, "A novel cerclage insertion: modified laparoscopic transabdominal cervical cerclage with transvaginal removing (MLTCC-TR)," *Journal of Minimally Invasive Gynecology*, vol. 27, no. 6, pp. 1300–1307, 2020.

[7] Y. E. Abdelhak, R. Aronov, H. Roque, and B. K. Young, "Management of cervical cerclage at term: remove the suture in labor," *Journal of Perinatal Medicine*, vol. 28, no. 6, pp. 453–457, 2000.

[8] M. Mönckeberg, R. Valdés, J. P. Kusanovic et al., "Patients with acute cervical insufficiency without intra-amniotic infection/inflammation treated with cerclage have a good prognosis," *Journal of Perinatal Medicine*, vol. 47, no. 5, pp. 500–509, 2019.

[9] S. Huang, N. Cai, P. P. Pacheco, S. Narrandes, Y. Wang, and W. Xu, "Applications of support vector machine (SVM) learning in cancer genomics," *CANCER GENOMICS and PROTEOMICS*, vol. 15, no. 1, pp. 41–51, 2018.

[10] M. Chu, X. Liu, R. Gong, and J. Zhao, "Support vector machine with quantile hyper-spheres for pattern classification," *PLoS One*, vol. 14, no. 2, Article ID e0212361, 2019.

[11] A. Tabet, T. Gebhart, G. Wu et al., "Applying support-vector machine learning algorithms toward predicting host-guest interactions with cucurbit[7]uril," *Physical Chemistry Chemical Physics*, vol. 22, no. 26, pp. 14976–14982, 2020.

[12] Z. Lv and L. Qiao, "Analysis of healthcare big data," *Future Generation Computer Systems*, vol. 109, pp. 103–110, 2020.

[13] Y. Li, J. Zhao, Z. Lv, and J. Li, "Medical image fusion method by deep learning," *International Journal of Cognitive Computing in Engineering*, vol. 2, pp. 21–29, 2021.

[14] Y. Han, M. Li, H. Ma, and H. Yang, "Cervical insufficiency: a noteworthy disease with controversies," *Journal of Perinatal Medicine*, vol. 48, no. 7, pp. 648–655, 2020.

[15] S. Xie, Z. Yu, and Z. Lv, "Multi-disease prediction based on deep learning: a survey," *Computer Modeling in Engineering and Sciences*, vol. 128, no. 2, pp. 489–522, 2021.

[16] C. Guo, J. Lu, Z. Tian, W. Guo, and A. Darvishan, "Optimization of critical parameters of PEM fuel cell using TLBO-DE based on Elman neural network," *Energy Conversion and Management*, vol. 183, pp. 149–158, 2019.

[17] S. Guo, R. Chen, H. Li, T. Zhang, and Y. Liu, "Identify severity bug report with distribution imbalance by CR-SMOTE and

ELM," *International Journal of Software Engineering and Knowledge Engineering*, vol. 29, no. 2, pp. 136–175, 2019.

[18] P. Černohorská, H. Vitásková, Z. Kokrdová, Z. Hájek, M. Koucký, and A. Pařízek, "Cervical cerclage - history and contemporary use," *Ceská Gynekologie*, vol. 84, no. 1, pp. 55–60, 2019.

[19] C. A. Enakpene, L. DiGiovanni, T. N. Jones, M. Marshalla, D. Mastrogiannis, and M. Della Torre, "Cervical cerclage for singleton pregnant patients on vaginal progesterone with progressive cervical shortening," *American Journal of Obstetrics and Gynecology*, vol. 219, no. 4, pp. e1–397, 2018 Oct.

[20] C. Y. Akladios, N. Sananes, A. Gaudineau, E. Boudier, and B. Langer, "Le cerclage cervical," *Journal de Gynécologie Obstétrique et Biologie de la Reproduction*, vol. 44, no. 8, pp. 771–775, 2015.

[21] R. Brown, R. Gagnon, and M.-F. Delisle, "No. 373-Cervical insufficiency and cervical cerclage," *Journal of Obstetrics and Gynaecology Canada*, vol. 41, no. 2, pp. 233–247, 2019.